Food Chemistry 141 (2013) 3731–3737

Contents lists available at SciVerse ScienceDirect

Food Chemistry

journal homepage: www.elsevier.com/locate/foodchem

Electrochemical sensor based on graphene and mesoporous TiO_2 for the simultaneous determination of trace colourants in food

Tian Gan *, Junyong Sun, Wen Meng, Li Song, Yuxia Zhang

College of Chemistry and Chemical Engineering, Xinyang Normal University, Xinyang 464000, China

ARTICLE INFO

Article history:
Received 24 March 2013
Received in revised form 13 June 2013
Accepted 18 June 2013
Available online 28 June 2013

Keywords:
Graphene
Mesoporous TiO_2
Sunset yellow
Tartrazine
Electrochemical sensor
Simultaneous determination

ABSTRACT

Currently, synthetic colourants draw much attention as food additives. This paper investigated the simultaneous electrocatalytic oxidation of sunset yellow and tartrazine, two yellow colourants commonly present in food together, with a novel voltammetric sensor based on graphene and mesoporous TiO_2 modified carbon paste electrode. Due to the high accumulation effect and great catalytic capability of graphene and mesoporous TiO_2, the developed sensor exhibited well-defined and separate square wave voltammetric peaks (i.e., 272 mV) for sunset yellow tartrazine. The peak currents of sunset yellow and tartrazine increased linearly with their concentration in the ranges of 0.02–2.05 μM and 0.02–1.18 μM, respectively. And the detection limit was 6.0 and 8.0 nM for sunset yellow and tartrazine, respectively. This new sensor was applied to determine sunset yellow and tartrazine in several food sample extracts. Results suggested that the proposed sensor was sensitive, rapid and reliable.

1. Introduction

Synthetic colourants have been used to replace natural ones for many years in the food industry, because they show many advantages such as high stability to light, oxygen and pH, colour uniformity, low microbiological contamination, relative lower production costs, and so on (Zhang, Zhang, Lu, Yang, & Wu, 2010; Zhang, Gan, Wan, & Wu, 2013; Wang et al., 2010). But nowadays, using many of them that contain azo groups gives rise to serious reservations concerning health. For example, recent studies show that sunset yellow and tartrazine can cause the appearance of allergies and asthma (Nevado, Flores, & Llerena, 1997) and childhood hyperactivity (Silva, Garcia, Lima, & Barrado, 2007). In Europe, the use of colourants in food products is regulated by the "Food Colour Directive" 94/36/EC dated 26 July 1995 (Małgorzata, Zofia, Małgorzata, & Elżbieta, 2005). In China, the sunset yellow and tartrazine can be used as food additives at a maximum limit of 0.5 and 0.1 g/kg, respectively (GB2760-1996). Facing with increasing legal restrictions, food dye determination became an analytical challenge. Until now, studies of colourants in food products have mainly been carried out using chromatographic method (Alves, Brum, de Andrade, & Netto, 2008) and spectrophotometric method (Oakley, Fabian, Mayhew, Svoboda, & Wustholz, 2012). But the electrochemical techniques with the advantages of simplicity, convenience, speediness and friendly to environment, have caused more and more attention (Medeiros, Lourencao, Rocha, & Fatibello, 2012; Gan et al., 2012; Ghoreishi, Behpour, & Golestaneh, 2012; Zhang, Liu, Zheng, Huang, & Wan, 2009).

Graphene, a single sheet of carbon atoms arranged in a honeycomb lattice, has generated a frenzy of research activity in recent years and in turn considerable speculation on its potential applications (Hla, 2012). For applications in electrochemical sensing, lots of substances have been detected including phytohormone (Gan, Hu, Chen, & Hu, 2011), biomoleculars (Huang et al., 2012), pharmaceuticals (Wei et al., 2012), toxic food additives (Wu, Sun, Li, & Wu, 2012), environmental pollutants (Gan, Sun, Huang, Song, & Li, 2012), and so on. All of these reports showed an interesting potential of graphene as a sensitizing material. Mesoporous materials are characterized by their high surface area. Three grams of this material contains as much surface area as a football field (Anuradha & Ranganathan, 1999). As a new class of this material, mesoporous transition metal oxides, like Co_3O_4 (Wang, Wu, Wu, Cheng, & Zhou, 2012), TiO_2 (Li et al., 2011), MnO_2 (Gan et al., 2012) have exhibited great interest in catalysis because of their large and uniform pore sizes. Among them, mesoporous TiO_2 is important because it is innocuous and can serve as support for conductive material, leading to quantum wires for smart electronic devices. For example, Lunsford et al. fabricated a sonogel carbon electrode modified with mesoporous TiO_2 for the determination of catechol (Lunsford, Choi, Stinson, Yeary, & Dionysiou, 2007). Xie et al. used mesoporous TiO_2-modified electrode to determine hypoxanthine based on enhanced voltammetric response (Xie, Yang, & Sun, 2008). And a phenols electrochemical sensor was developed by Lin et al. using

* Corresponding author. Tel.: +86 376 6390702; fax: +86 376 6390597.
E-mail address: gantianxynu@163.com (T. Gan).

0308-8146/$ - see front matter © 2013 Elsevier Ltd. All rights reserved.
http://dx.doi.org/10.1016/j.foodchem.2013.06.084

mesoporous TiO_2 nanoparticles based carbon paste electrodes (Lin et al., 2009).

Because of the importance of determination of sunset yellow and tartrazine considering food safety, in this work we fabricated one electrochemical sensor based on graphene and mesoporous TiO_2 nanomaterials modified carbon paste electrode to investigate the voltammetric behaviours of sunset yellow and tartrazine, with the aim of developing their simple, rapid and simultaneous determination at low concentration levels using square wave voltammetry. This novel sensor owns wider peak-to-peak separation between sunset yellow and tartrazine (i.e., 272 mV) and lower detection limit (i.e., 6.0 nM for sunset yellow and 8.0 nM for tartrazine) compared with the reported electrochemical sensors based on solid state working electrode (Table 1). Furthermore, to validate the proposed sensor, the determination of sunset yellow and tartrazine in the samples of candy, royal jelly, ice cream, solid custard jelly, juice powder, soft drink and colouring coated chocolate was performed and the obtained results were compared with that from high performance liquid chromatography (HPLC).

2. Experimental

2.1. Reagents

Sunset yellow and tartrazine were obtained from Sigma, and individually dissolved into double distilled water to prepare 1.0 g L^{-1} standard solution. Graphite powder (spectral pure), H_2SO_4, $K_2S_2O_8$, P_2O_5, H_2O_2, HCl, $KMnO_4$, $NaBH_4$, titanium butoxide ($Ti(OBu)_4$) and hexadecyl trimethyl ammonium bromide (CTAB) (analytical grade) were purchased from Sinopharm Chemical Reagent (Shanghai, China). All chemicals were used as received, and the water was double distilled.

2.2. Instruments

Electrochemical measurements were performed on a CHI 660D electrochemical workstation (Chenhua Instrument, Shanghai, China) with a conventional three-electrode system. The working electrode is the colourants sensor (graphene and mesoporous TiO_2 nanomaterials modified carbon paste electrode), the reference electrode is a saturated calomel electrode (SCE), and the counter electrode is a platinum wire. Scanning electron microscopy (SEM) and energy dispersive spectroscopy (EDS) were conducted with a Quanta 450 microscope (FEI Company, Holland). Transmission electron microscopy (TEM) images were obtained on TECNAI G2 20 S-TWIN transmission electron microscope (FEI Company, Holland).

2.3. Preparation of graphene and mesoporous TiO_2

Graphene oxide was prepared from natural graphite flakes by Hummer's method (Sreeprasad, Samal, & Pradeep, 2009), and was then reduced by $NaBH_4$ in a steam bath to produce the graphene (GN) (Bourlinos et al., 2003). Mesoporous TiO_2 was synthesized according to the report (Li, Zhuang, Li, & Pan, 2012), which used $Ti(OBu)_4$ as the source of Ti, and CTAB as the organic template. The ordered mesopores could be formed in TiO_2 nanoparticles by calcining at 400 °C for 8 h to remove the organic template.

2.4. Fabrication of the electrochemical sensor

Graphene (0.20 g), mesoporous TiO_2 (0.20 g) and graphite powder (1.0 g) were exactly weighed and put in a carnelian mortar. The total mass ratio of graphene, mesoporous TiO_2 and graphite was controlled to 1:1:5. After that, 0.35 mL paraffin oil was added into the powder and then mixed homogeneously. Finally, the resulting carbon paste was tightly pressed into the end cavity of a carbon paste electrode (CPE) body, and the electrode surface (3-mm in diameter) was polished on a smooth paper, and denoted as colourants sensor or GN/TiO_2-CPE. The GN modified CPE (GN-CPE) and mesoporous TiO_2 modified CPE (TiO_2-CPE) were prepared by the same procedure only using GN or mesoporous TiO_2, and the mass ratio of GN or mesoporous TiO_2 to graphite powder was 1:5. And the unmodified CPE was also prepared without addition of GN or mesoporous TiO_2.

2.5. Cyclic and square wave voltammograms

Cyclic voltammograms (CV) were recorded in the 0.4–1.1 V for sunset yellow and 0.8–1.3 V for tartrazine, respectively at different scan rates from 100 to 400 mV s^{-1} in 0.1 M H_2SO_4 without accumulation. Square wave voltammograms (SWV) were obtained at a potential window of 0.4–1.15 V after 2-min accumulation. The oxidation peak current at 0.805 and 1.076 V was individually measured for sunset yellow and tartrazine. The amplitude is 40 mV and the frequency is 20 Hz.

2.6. Sample preparation and detection

Candy, royal jelly, ice cream, solid custard jelly powder, juice powder, soft drink and colouring coated chocolate were selected as detection samples in this work based on the published work (Sahraei, Farmany, & Mortazavi, 2013; Tripathi, Khanna, & Das, 2004) because sunset yellow and tartrazine may be added into them to improve their yellow colour. These seven samples were purchased from the local super market and were changed into solution as follows. 5.7199-g candy, 10.0742-g royal jelly, 30.0512-g ice cream, 8.8974-g solid custard jelly powder and 8.7423-g juice powder were respectively dissolved in hot pure water (~45 °C), diluted to 100 mL and filtered through a 0.45 μm membrane filter to obtain solution without precipitation for subsequent use (Shawish, Ghalwa, Saadeh, & Harazeen, 2013). Soft drink sample was used directly without any pretreatment. 5 pieces of (5.2411 g) of colouring coated chocolates were added in distilled

Table 1
Comparison of the analytical performance between this sensor and the reported electrochemical sensors based on solid state working electrode.

Analyte	Working electrode	Peak separation (mV)	Linear range (nM)	Limit of detection (nM)	Reference
Sunset yellow	Pretreated boron-doped diamond electrode	150	20.0–4760	13.1	Medeiros et al. (2012)
Tartrazine			99.9–5660	62.7	
Sunset yellow	Graphene–phosphotungstic acid/GCE	260	33.2–464	1.1	Gan et al. (2012)
Tartrazine			112–2810	56.1	
Sunset yellow	Au NPs/CPE	25	100.0–2000	30.0	Ghoreishi et al. (2012)
Tartrazine			50.0–1600	2.0	
Sunset yellow	MWNT/GCE	250	55.3–110,000	22	Zhang et al. (2009)
Tartrazine			374–748,000	188	
Sunset yellow	GN/TiO_2-CPE	272	20–2050	6.0	This work
Tartrazine			20–1180	8.0	

water and after dissolving coloured shell; the remained solution was separated, centrifuged and diluted with an equal volume of 3 M CH_3COOH solution. 200 mg of white commercial wool yarn, washed with detergent and distilled water and dried, were added to 10 mL chocolate sample and the mixture was heated for a period of 60 min at 60 °C. Then the coloured yarn was taken out of the solution and washed with a plenty of distilled water. The dyes were recovered by mixing the yarn with 10 mL 2 M NH_3 and heating for 10 min at 90 °C (Sorouraddin, Rostami, & Saadati, 2011).

When detecting sunset yellow and tartrazine using the colourants sensor, a 0.1 mL sample extract was added into 5.0 mL H_2SO_4 (0.1 M), and then analyzed according to the analytical procedure. In addition, HPLC (Agilent 1100 Series, USA) was also used to detect sunset and tartrazine in sample extracts according to Alves et al., (2008). The column was a C18 analytical column (4.6 mm × 250 mm × 5 μm). Two different mobile phase systems were employed to accomplish a quick separation of the analyzed dyes in samples. System I consisted of methanol (solution A) and 0.08 M aqueous ammonium acetate (solution B). System II consisted of methanol (solution A) and an aqueous solution containing 5 mM EDTA and 30 mM sodium acetate with a final pH adjusted to 3.5 with addition of diluted acetic acid (solution B). The aqueous solutions and methanol were degassed in ultrasonic bath and further filtered through 0.45 μm membranes prior to use. Isocratic conditions were employed for both solvent systems and the mobile phase was composed of 45% of solution A and 55% of solution B. A constant flow rate of 1.0 mL min^{-1} was used, and the sample injection volume was 20 μL. The detection was performed at a wavelength of 417 nm for sunset yellow and 426 nm for tartrazine with UV–vis spectra detector.

3. Results and discussion

3.1. Characterization of graphene and mesoporous TiO_2

The morphology, constitution and microstructure of graphene and mesoporous TiO_2 were examined by SEM, TEM and EDS, respectively. In Fig. 1a, SEM observation shows the folding structure at the edges of the graphene, suggesting a very small thickness. SEM image of mesoporous TiO_2 clearly illustrate that TiO_2 nanoparticles are distributed individually with legible boundary lines (Fig. 1b). Furthermore, low magnification of TEM image testify the mono-dispersibility of mesoporous TiO_2 nanoparticles, they are so uniform that no aggregated or free nanoparticles were detected (Fig. 1c). In order to probe the subtle structure of TiO_2 particles, a TEM image with high magnification was also obtained (Fig. 1d). From which it can be seen that the inner of TiO_2 nanoparticles were fully distributed with continuous and ordered mesoporous channels, which can increase the effective surface area of TiO_2 nanoparticles superiorly. The EDS image of mesoporous TiO_2 shows the existence of C, Ti and O elements in the resulting TiO_2 material (Fig. 1e). The peak of C element is caused by the conductive substrate when conducting EDS. This result further confirms the component of the synthesized TiO_2 and therefore the successful preparation of TiO_2. Based on the former images, the possible simulative framework of GN/TiO_2 carbon paste was presented as Fig. 1f.

3.2. Electrochemical behaviours of sunset yellow and tartrazine at this sensor

The utility of this colourants sensor for the oxidation of sunset yellow was evaluated by cyclic voltammetry. The cyclic voltammetric response of an unmodified CPE in 0.1 M H_2SO_4 is shown as curve a in Fig. 2A. Sunset yellow was oxidized at around 0.913 V with a peak current of 0.710 μA during the process from 0.4 to 1.1 V, and on the reverse scan, it was reduced at about 0.837 V with an obtuse protuberance. However, the oxidation of sunset yellow at the GN/TiO_2 modified CPE was around 0.878 V with a peak current of 3.49 μA and the corresponding reduction peak was more evident compared to that on unmodified CPE, but was still not symmetrical to the oxidation peak (curve b). Evidently, the redox of sunset yellow was not a full reversible process, and the oxidation peak was selected as the determination signal in subsequent experiment because it was more evident. In addition, a decrease in overpotential and an enhancement of peak current for sunset yellow oxidation were achieved at the modified electrode due to the high surface area and catalytic ability of graphene and mesoporous TiO_2. Therefore, the sensitivity can be improved greatly for the determination of sunset yellow, and the lower oxidation potential can avoid the co-oxidation of other interferences that may coexist in food samples with sunset yellow.

To understand the electrochemical behaviour of tartrazine at unmodified CPE and GN/TiO_2 modified CPE, its cyclic voltammograms were also examined in 0.1 M H_2SO_4 at a scan rate of 150 mV s^{-1} (Fig. 2B). As shown in curve c, tartrazine showed an irreversible weak oxidation peak at 1.173 V at the unmodified CPE due to the sluggish electron transfer kinetics of tartrazine oxidation process, which may be related to the electron fouling caused by the deposition of tartrazine and its oxidation products on the electrode surface. It could be found from curve d that the electron-oxidation of tartrazine on the GN/TiO_2 modified CPE showed

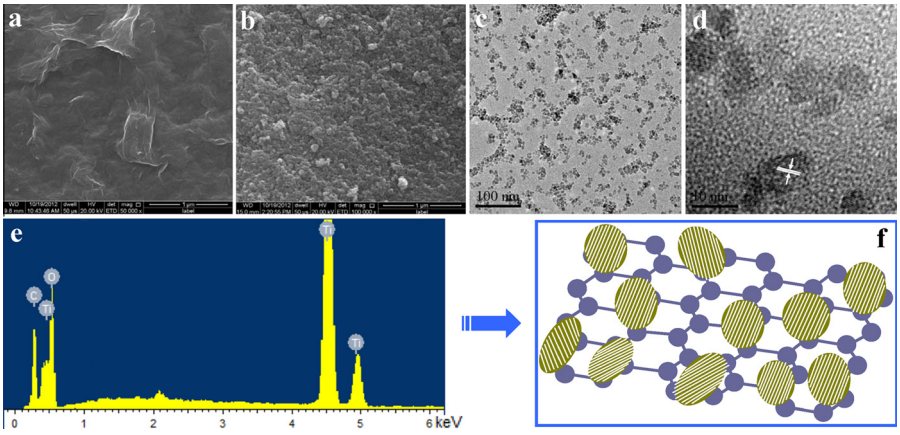

Fig. 1. (a) and (b) Depict the SEM images of graphene and mesoporous TiO_2, respectively. (c) and (d) The TEM images of mesoporous TiO_2 with low and high magnification, respectively. (e) and (f) EDS image and the simulative framework of GN/mesoporous TiO_2 material, respectively.

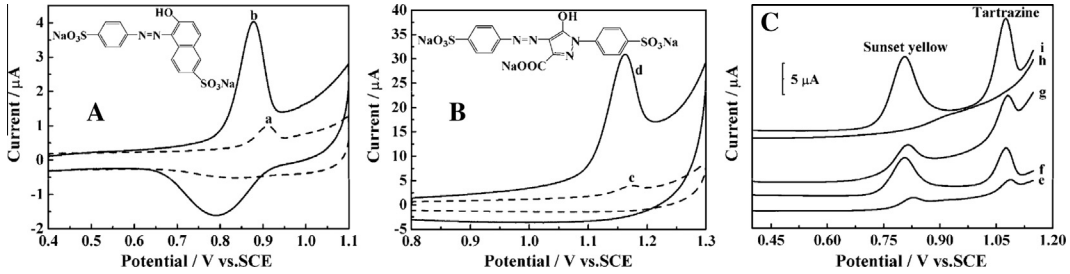

Fig. 2. (A) The CVs of 1.0 μM sunset yellow at (a) unmodified CPE and (b) GN/TiO_2-CPE. Scan rate is 200 mV s^{-1}. (B) The CVs of 5.0 μM tartrazine at (c) unmodified CPE and (d) GN/TiO_2-CPE. Scan rate is 150 mV s^{-1}. (C) The SWV curves of 0.5 μM sunset yellow and 0.8 μM tartrazine on the unmodified CPE (e), GN-CPE (f), TiO_2-CPE (g) and GN/TiO_2-CPE (i). Curve h depicts the GN/TiO_2-CPE in 0.1 M H_2SO_4. Accumulation time: 2 min.

a sharp anodic peak at 1.163 V and the anodic peak current was enhanced by about 10.8-fold in comparison with the anodic peak current on the unmodified CPE. As compared to the unmodified CPE, the observed negatively shifted peak potential and enhanced peak current for the oxidation of tartrazine at the GN/TiO_2 modified CPE indicated that the graphene and mesoporous TiO_2 showed excellent electrocatalytic activity and accumulation capability toward the oxidation of tartrazine.

3.3. Square wave voltammetric analysis

The electrochemical behaviours of sunset yellow and tartrazine were studied using SWV on the unmodified CPE, GN modified CPE, TiO_2 modified CPE and GN/TiO_2 modified CPE. Fig. 2C displays the oxidation responses of 0.5 μM sunset yellow and 0.8 μM tartrazine in 0.1 M H_2SO_4. After 2-min accumulation under open-circuit, two small oxidation peaks were observed on the unmodified CPE (curve e). The low peak currents of 1.08 μA for sunset yellow and 1.30 μA for tartrazine indicate that the oxidation activity of them are very diminutive on the unmodified CPE surface. When using GN modified CPE (curve f) and TiO_2 modified CPE (curve g), the oxidation signals of sunset yellow and tartrazine both had an increase of about 4 times. And the peak potentials of sunset yellow and tartrazine shifted negatively about 20 and 10 mV, respectively. However, the best electrocatalytic oxidation of sunset yellow and tartrazine could be achieved on GN/TiO_2 modified CPE (curve i) because two well-defined oxidation peaks could be seen clearly. The oxidation peaks were at 0.804 and 1.076 V, and the peak potential difference was 272 mV. Compared with unmodified CPE, GN modified CPE and TiO_2 modified CPE, GN and TiO_2 together are more active for the simultaneous electrochemical oxidation and detection of sunset yellow and tartrazine. This may be caused by the cumulate accumulation capability and catalytic effect of graphene and mesoporous TiO_2 which will lead to accelerated electrons transfer of the analytes. Furthermore, the SWV curve of GN/TiO_2 modified CPE in 0.1 M H_2SO_4 was smooth with no evident peak (curve h), so the peaks belong to the oxidation of sunset yellow and tartrazine authentically.

3.4. Optimization studies

The effects of several parameters, such as the electrolyte, composition of carbon paste, scan rate, accumulation time and potential on the voltammetric responses of sunset yellow and tartrazine using this sensor were investigated.

The electrochemical responses of 0.5 μM sunset yellow and 0.8 μM tartrazine at this sensor in different supporting electrolytes such as disodium hydrogen phosphate–citric acid buffer solution (pH 2.2, 3.6, 4.4, 7.0 and 8.0), 0.2 M sodium acetate–acetic acid buffer solution (pH 2.6, 4.0, 4.4 and 5.4), boric acid–borax buffer solution (pH 7.4, 8.0, 8.4 and 9.0), 0.1 M phosphate buffer solution (pH 5.8, 6.5, 7.0 and 8.0) and 0.1 M HCl, H_2SO_4, $HClO_4$, NaOH solution were examined by SWV. It was found that no redox peaks was observed in alkaline electrolytes, and only two small oxidation peaks were found in neutral and weak acid environment. But evident peaks could be obtained in strong acid electrolytes, like 0.1 M HCl, H_2SO_4 and $HClO_4$, and the best voltammogram shape in 0.1 M H_2SO_4. Thus, 0.1 M H_2SO_4 solution was chosen as the electrocatalytic medium for the simultaneous oxidation of sunset yellow and tartrazine.

The mass ratio of graphene and TiO_2 in the carbon paste has a significant influence on the voltammetric responses of sunset yellow and tartrazine. When changing the mass ratio of graphene:mesoporous TiO_2:graphite from 1:1:7, 1:1:6, 1:1:5, 1:1:4, 1:2:5, 1:3:5, 2:1:5 to 3:1:5, the highest peak could be obtained when the mass ratio is 1:1:5. Less graphene and mesoporous TiO_2 content may reduce the effective electrode surface area, which may weaken the accumulation ability of this sensor. However, less conductive graphite content may lower the conductivity of the modified electrode. So the mass ratio of graphene:mesoporous TiO_2:graphite was chosen as 1:1:5.

The influence of scan rate on the oxidation current of sunset yellow and tartrazine on this sensor was examined. The oxidation peak currents of sunset yellow and tartrazine linearly increased with the square root of scan rate in the range of 100–400 mV s^{-1}, indicating diffusion-controlled electrode processes of them. Meanwhile, the oxidation peak potential (E_p, V) of sunset yellow (Fig. 3A) and tartrazine (Fig. 3B) positively shifted with scan rate (v, mV s^{-1}) according to the following regression:

$$E_p = 0.743 + 0.0257 \ln v (r^2 = 0.995, \text{sunset yellow}) \quad (1)$$

$$E_p = 1.038 + 0.0250 \ln v (r^2 = 0.995, \text{tartrazine}) \quad (2)$$

For a diffusion-controlled electrode process, the relationship between E_p and v is in accordance with the following equation (Bard & Faulkner, 1980):

$$E_p = E^{0'} + \left(\frac{RT}{\alpha nF}\right)\left[0.780 + \ln\left(\frac{D_R^{1/2}}{k^0}\right) + \ln\left(\frac{\alpha nFv}{RT}\right)^{1/2}\right] = K + \frac{RT}{2\alpha nF}\ln v \quad (3)$$

where k^0 is the standard rate constant of the surface reaction, $E^{0'}$ is the formal potential, α is transfer coefficient of the oxidation of sunset yellow and tartrazine, and other symbols have their usual meanings. According to Eq. (3), the electron transfer number (n) of sunset yellow and tartrazine can be calculated from the plot of E_p vs. ln$v$, i.e., one electron is involved in both of the electrochemical oxidation of sunset yellow and tartrazine. The possible electrochemical reaction mechanism of sunset yellow and tartrazine were put forward in Fig. 3 C and D based on our previous word (Gan et al., 2012).

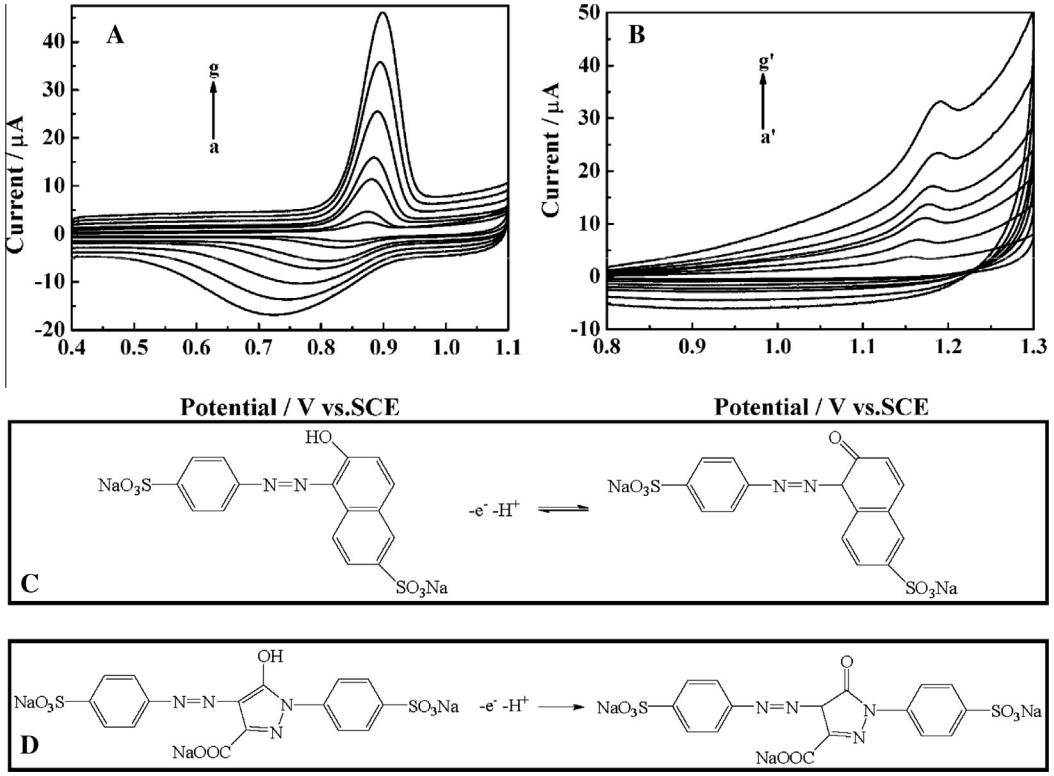

Fig. 3. Cyclic voltammograms of 3.0 μM sunset yellow (A) and 0.5 μM tartrazine (B) in 0.1 M H_2SO_4 at GN/TiO_2-CPE with different scan rates: 100 (a,a′), 150 (b,b′), 200 (c,c′), 250 (d,d′), 300 (e,e′), 350 (f,f′), 400 (g,g′). And the possible electrochemical reaction mechanism of sunset yellow (C) and tartrazine (D).

The oxidation peak current of sunset yellow and tartrazine under different potential were measured to evaluate the influence of accumulation potential. The time was 2 min, and the studied accumulation potential were 0.2, 0.3, 0.4, 0.5, 0.6 and 0.7 V. Moreover, the accumulation step was also conducted under open-circuit. It was found that the oxidation peak current of 0.5 μM sunset yellow and 0.8 μM tartrazine almost kept unchanged, suggesting no influence of accumulation potential on the detection of sunset yellow and tartrazine. Herein, the accumulation step was performed under open-circuit. The influence of accumulation time on the oxidation peak current of sunset yellow and tartrazine was also investigated. By extending the accumulation time from 0 to 2 min, the oxidation peak current greatly increased. This phenomenon suggests that accumulation is efficient to improve the detection sensitivity. Longer accumulation time than 2 min did not enhance the oxidation peak current, indicating that the amount of sunset yellow and tartrazine on the surface of this sensor tends to a limiting value. Considering sensitivity and analysis time, 2-min accumulation was employed.

3.5. Calibration, reproducibility and selectivity

SWV was used to determine the calibration plots and detection limit for sunset yellow and tartrazine. As can be seen from inserts of Fig. 4A and B, the peak currents of SWVs increased with increasing the concentration of sunset yellow (tartrazine) even in the presence of tartrazine (sunset yellow). The obtained voltammograms in Fig. 4A clearly showed that 0.8 μM tartrazine had no interference with the determination of sunset yellow in the range of 0.02 to 2.05 μM (curves a–j). In addition, it could be found in Fig. 4B that 0.25 μM sunset yellow did not affect the detection of tartrazine, too. And the calibration plot for tartrazine between 0.02 and 1.18 μM could be obtained (curves a′–j′). The detection limit (3σ) was calculated as 6.0 nM for sunset yellow and 8.0 nM for tartrazine.

The successive measurements using one colourant sensor were examined in sunset yellow and tartrazine binary mixed solution. Unfortunately, the oxidation peak currents of sunset yellow and tartrazine decreased continuously, most likely due to the surface adsorption of the oxidation products of sunset yellow and tartrazine. But the constant peak currents of sunset yellow and tartrazine could be obtained when the surface graphene–mesoporous TiO_2 paste was rubbed and polished with new graphene–mesoporous TiO_2 paste again. The reproducibility between multiple sensors with successive newly fabricated surface was then evaluated by parallel determination of the oxidation peak current of 0.5 μM sunset yellow and 0.8 μM tartrazine. The relative standard deviation (RSD) is 2.7% for 10 sensors, indicative of an excellent fabrication reproducibility and detection precision.

The influence of various foreign species on the determination of sunset yellow and tartrazine was studied. The tolerance limit was taken as the maximum concentration of the foreign substances, which caused an approximiately ±6% relative error in the determination of these two substances. No influence on the detection of 0.2 μM sunset yellow and tartrazine was found after the addition of 1000-fold concentrations of glucose, sucrose and glycine; 500-fold concentrations of citric acid; 300-fold concentrations of vitamin C; 100-fold concentrations of Fe^{3+}, Ca^{2+}, Cu^{2+}, Mg^{2+}; or 50-fold concentrations of ponceau 4R, amaranth, allura red and quinoline yellow.

3.6. Practical application

In order to evaluate the performance of this sensor in real samples, it was used to determine sunset yellow and tartrazine in candy, royal jelly, ice cream, solid custard jelly powder, juice powder, soft drink and colouring coated chocolate samples. Typical results can be seen in Table 2, which were obtained by the standard addition method. In order to test the accuracy of this sensor, the contents of sunset yellow and tartrazine were also analyzed by

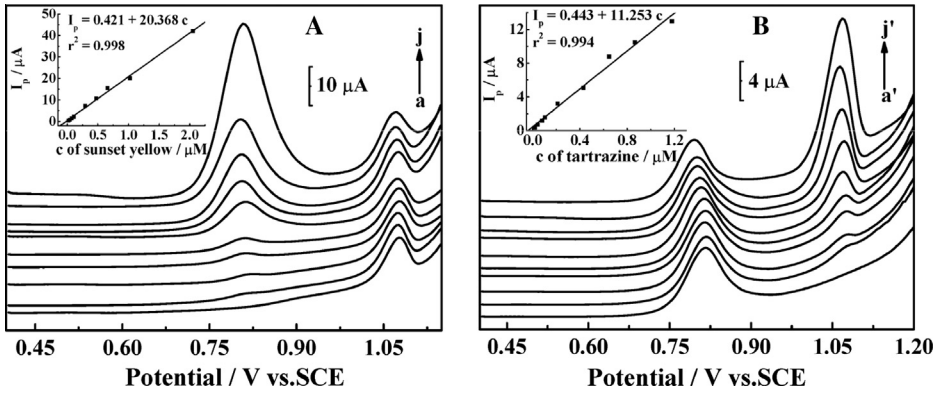

Fig. 4. (A) The SWV graphs of (a) 0, (b) 0.02, (c) 0.04, (d) 0.07, (e) 0.11, (f) 0.29, (g) 0.48, (h) 0.66, (i) 1.02 and (j) 2.05 μM sunset yellow in 0.1 M H_2SO_4 at GN/TiO_2-CPE in the presence of 0.8 μM tartrazine. Insert: linear range of the peak current vs. the concentration of sunset yellow. (B) The SWV graphs of (a′) 0, (b′) 0.02, (c′) 0.04, (d′) 0.08, (e′) 0.11, (f′) 0.21, (g′) 0.43, (h′) 0.65, (i′) 0.87 and (j′) 1.18 μM tartrazine in 0.1 M H_2SO_4 at GN/TiO_2-CPE in the presence of 0.25 μM tartrazine. Insert: linear range of the peak current vs. the concentration of tartrazine. Accumulation time: 2 min.

Table 2
Simultaneous determination of sunset yellow and tartrazine in food sample extracts.

Sample	Analytes	By this method[a] (nM)	By HPLC[a] (nM)	Rel error (%)	RSD (%)	Added (nM)	Found (nM)	Recovery (%)
Candy	Sunset yellow	100.43	100.57	−0.14	4.0	100.00	98.98	98.98
	Tartrazine	100.29	100.10	0.19	3.2	100.00	102.14	102.1
Royal jelly	Sunset yellow	21.71	20.70	4.88	3.4	20.00	19.76	98.80
	Tartrazine	65.24	66.08	−1.27	2.4	65.00	64.61	99.40
Ice cream	Sunset yellow	105.11	105.48	−0.32	3.7	100.00	100.27	100.3
	Tartrazine	220.33	220.72	−0.17	4.2	220.00	219.18	99.63
Solid custard jelly	Sunset yellow	78.58	77.99	0.76	2.6	80.00	79.81	99.76
	Tartrazine	0.00	0.00			80.00	81.02	101.3
Juice powder	Sunset yellow	300.10	299.37	0.24	2.7	300.00	300.72	100.2
	Tartrazine	247.25	248.26	−0.41	3.3	250.00	248.95	99.58
Soft drink	Sunset yellow	174.21	175.07	−0.49	3.6	170.00	167.98	98.81
	Tartrazine	168.55	169.02	−0.28	2.9	170.00	172.31	101.4
Colouring coated chocolate	Sunset yellow	0.00	0.00			60.00	57.69	96.15
	Tartrazine	62.13	63.52	−2.19	4.7	60.00	58.45	97.41

[a] Values reported are mean of six replicates.

HPLC. The results obtained by HPLC and this sensor are in good agreement, revealing that this sensor is satisfactory. In addition, known amounts of sunset yellow and tartrazine were spiked in the samples, and then analyzed according to the same procedure. The value of recovery is between 96.15% and 102.1%, also indicating the fabricated sensor represents a good and easy way for monitoring sunset yellow and tartrazine in real samples.

4. Conclusions

In conclusion, the results indicate that square wave voltammetry represents a fast and relatively low-cost technique for simultaneous measuring the sunset yellow and tartrazine in food samples, given the high accumulation ability, strong catalytic property and excellent sensitivity of the electrochemical sensor based on graphene and mesoporous TiO_2 modified carbon paste electrode. The practical usefulness of the sensor was demonstrated by the estimation of the content of sunset yellow and tartrazine in real food samples, using an extremely simple procedure involving the direct addition of sample extracts into the electrochemical cell, dispensing with any sample pretreatment.

Acknowledgements

We gratefully acknowledge financial support from National Natural Science Foundation of China (No. 61201091), the Project of Science and Technology development of Henan Province (Nos. 0124020221, 0624440065) and the Program for University Innovative Research Team of Henan (No. 2012IRTSHN017).

References

Alves, S. P., Brum, D. M., de Andrade, E. C. B., & Netto, A. D. P. (2008). Determination of synthetic dyes in selected foodstuffs by high performance liquid chromatography with UV–DAD detection. *Food Chemistry, 107*(1), 489–496.

Anuradha, T. V., & Ranganathan, S. (1999). Synthesis of mesoporous matemals based on titanium(IV)oxide and titanium nitride. *Nanostructured Materials, 12*(5–8), 1063–1069.

Bard, A. J., & Faulkner, L. R. (1980). *Electrochemical methods fundamentals and applications*. New York: Wiley.

Bourlinos, A. B., Gournis, D., Petridis, D., Szabó, T., Szeri, A., & Dékány, I. (2003). Graphite oxide: Chemical reduction to graphite and surface modification with primary aliphatic amino acids. *Langmuir, 19*(15), 6050–6055.

Gan, T., Hu, C. G., Chen, Z. L., & Hu, S. S. (2011). A disposable electrochemical sensor for the determination of indole-3-acetic acid based on poly(safranine T)-reduced graphene oxide nanocomposite. *Talanta, 85*(1), 310–316.

Gan, T., Sun, J. Y., Cao, S. Q., Gao, F. X., Zhang, Y. X., & Yang, Y. Q. (2012). One-step electrochemical approach for the preparation of graphene wrapped-phosphotungstic acid hybrid and its application for simultaneous determination of sunset yellow and tartrazine. *Electrochimica Acta, 74*, 151–157.

Gan, T., Sun, J. Y., Huang, K. J., Song, L., & Li, Y. M. (2012). A graphene oxide–mesoporous MnO_2 nanocomposite modified glassy carbon electrode as a novel and efficient voltammetric sensor for simultaneous determination of hydroquinone and catechol. *Sensors and Actuators B: Chemical, 177*, 412–418.

Ghoreishi, S. M., Behpour, M., & Golestaneh, M. (2012). Simultaneous determination of sunset yellow and tartrazine in soft drinks using gold nanoparticles carbon paste electrode. *Food Chemistry, 132*(1), 637–641.

Hla, S. W. (2012). Graphene: Conductivity measurements pick up. *Nature Nanotechnology, 7*, 693–694.

Huang, K. J., Miao, Y. X., Wang, L., Gan, T., Yu, M., & Wang, L. L. (2012). Direct electrochemistry of hemoglobin based on chitosan–ionic liquid–ferrocene/graphene composite film. *Process Biochemistry, 47*(7), 1171–1177.

Li, N., Liu, G., Zhen, C., Li, F., Zhang, L. L., & Cheng, H. M. (2011). Battery performance and photocatalytic activity of mesoporous anatase TiO_2 nanospheres/graphene composites by template-free self-assembly. *Advanced Functional Materials, 21*(9), 1717–1722.

Li, X. K., Zhuang, Z. J., Li, W., & Pan, H. Q. (2012). Photocatalytic reduction of CO_2 over noble metal-loaded and nitrogen-doped mesoporous TiO_2. *Applied Catalysis A: General, 429–430*, 31–38.

Lin, H. G., Ji, X. B., Chen, Q. Y., Zhou, Y. K., Banks, C. E., & Wu, K. B. (2009). Mesoporous-TiO_2 nanoparticles based carbon paste electrodes exhibit enhanced electrochemical sensitivity for phenols. *Electrochemistry Communications, 11*(10), 1990–1995.

Lunsford, S. K., Choi, H., Stinson, J., Yeary, A., & Dionysiou, D. D. (2007). Voltammetric determination of catechol using a sonogel carbon electrode modified with nanostructured titanium dioxide. *Talanta, 73*, 172–177.

Małgorzata, J., Zofia, S., Małgorzata, W., & Elżbieta, A. (2005). Separation of synthetic food colourants in the mixed micellar system: Application to pharmaceutical. *Journal of Chromatography A, 1081*(1), 42–47.

Medeiros, R. A., Lourencao, B. C., Rocha, R. C., & Fatibello, O. (2012). Simultaneous voltammetric determination of synthetic colorants in food using a cathodically pretreated boron-doped diamond electrode. *Talanta, 97*, 291–297.

Nevado, J. J. B., Flores, J. R., & Llerena, M. J. V. (1997). Adsorptive stripping voltammetry of tartrazine at the hanging mercury drop electrode in soft drinks. *Fresenius' Journal of Analytical Chemistry, 357*(7), 989–994.

Oakley, L. H., Fabian, D. M., Mayhew, H. E., Svoboda, S. A., & Wustholz, K. L. (2012). Pretreatment strategies for SERS analysis of indigo and prussian blue in aged painted surfaces. *Analytical Chemistry, 84*(18), 8006–8012.

Sahraei, R., Farmany, A., & Mortazavi, S. S. (2013). A nanosilver-based spectrophotometry method for sensitive determination of tartrazine in food samples. *Food Chemistry, 138*(2–3), 1239–1242.

Shawish, H. M., Ghalwa, N. A., Saadeh, S. M., & Harazeen, H. E. (2013). Development of novel potentiometric sensors for determination of tartrazine dye concentration in foodstuff products. *Food Chemistry, 138*(1), 126–132.

Silva, M. L. S., Garcia, M. B. Q., Lima, J. L. F. C., & Barrado, E. (2007). Voltammetric determination of food colourants using a polyallylamine modified tubular electrode in a multicommutated flow system. *Talanta, 72*(1), 282–288.

Sorouraddin, M. H., Rostami, A., & Saadati, M. (2011). A simple and portable multi-colour light emitting diode based photocolourimeter for the analysis of mixtures of five common food dyes. *Food Chemistry, 127*, 308–313.

Sreeprasad, T. S., Samal, A. K., & Pradeep, T. (2009). Tellurium nanowire-induced room temperature conversion of graphite oxide to leaf-like graphenic structures. *Journal of Physical Chemistry C, 113*(5), 1727–1737.

Tripathi, M., Khanna, S. K., & Das, M. (2004). A novel method for the determination of synthetic colors in ice cream samples. *Journal of AOAC International, 87*(3), 657–663.

Wang, P., Hu, X. Z., Cheng, Q., Zhao, X. Y., Fu, X. F., & Wu, K. B. (2010). Electrochemical detection of amaranth in food based on the enhancement effect of carbon nanotube film. *Journal of Agricultural and Food Chemistry, 58*(23), 12112–12116.

Wang, J. Q., Wu, C., Wu, K. B., Cheng, Q., & Zhou, Y. K. (2012). Electrochemical sensing chemical oxygen demand based on the catalytic activity of cobalt oxide film. *Analytica Chimica Acta, 736*, 55–61.

Wei, Q., Zhao, Y. F., Du, B., Wu, D., Li, H., & Yang, M. H. (2012). Ultrasensitive detection of kanamycin in animal derived foods by label-free electrochemical immunosensor. *Food Chemistry, 134*(3), 1601–1606.

Wu, C., Sun, D., Li, Q., & Wu, K. B. (2012). Electrochemical sensor for toxic ractopamine and clenbuterol based on the enhancement effect of graphene oxide. *Sensors and Actuators B: Chemical, 168*, 178–184.

Xie, X. F., Yang, K. F., & Sun, D. (2008). Voltammetric determination of hypoxanthine based on the enhancement effect of mesoporous TiO_2-modified electrode. *Colloids and Surfaces B: Biointerfaces, 67*(2), 261–264.

Zhang, Y. Y., Gan, T., Wan, C. D., & Wu, K. B. (2013). Morphology-controlled electrochemical sensing amaranth at nanomolar levels using alumina. *Analytica Chimica Acta, 764*, 53–58.

Zhang, W. K., Liu, T., Zheng, X. J., Huang, W. S., & Wan, C. D. (2009). Surface-enhanced oxidation and detection of sunset yellow and tartrazine using multi-walled carbon nanotubes film-modified electrode. *Colloids and Surfaces B: Biointerfaces, 74*(1), 28–31.

Zhang, Y., Zhang, X. J., Lu, X. H., Yang, J. Q., & Wu, K. B. (2010). Multi-wall carbon nanotube film-based electrochemical sensor for rapid detection of ponceau 4R and allura red. *Food Chemistry, 122*(3), 909–913.